Modeling and Optimization of Quasi-Phase Matching Via Domain-Disordering

Sean J. Wagner, *Member, IEEE*, Ahmed Al Muhairi, *Student Member, IEEE*, J.Stewart Aitchison, *Senior Member, IEEE*, and Amr S. Helmy, *Senior Member, IEEE*

***Abstract*—Second-harmonic generation in a quasi-phase matched waveguide produced using a domain-disordered GaAs–AlAs superlattice is modeled including the effects of group velocity mismatch, nonlinear refraction, two-photon absorption, and linear loss. The model predicts our experimentally observed second-harmonic powers within an order of magnitude. Self-phase modulation and two-photon absorption led to reduced conversion efficiencies of up to 33% at input peak powers >50 W. Group velocity mismatch results in a reduction of 23% in conversion efficiency using estimated group velocities calculated from the measured effective refractive index. The modeling also shows that the conversion efficiency peaks at propagation lengths longer than the pulse walk off length and that duty cycle variations induced shifts in the tuning curves. Group velocity mismatch also increased the conversion bandwidth by $\sim 30\%$. Incomplete modulation of $\chi^{(2)}$ in disordered regions reduced the output conversion efficiency by up to two orders of magnitude. Grating-assisted phase matching led to a 7% efficiency drop for a Δn of 0.045 at the second-harmonic and 0.01 at the fundamental. This model serves as a valuable tool to provide insight into the optimization of these devices.**

***Index Terms*—Integrated optics, nonlinear optics, optical phase matching, optical waveguides.**

I. Introduction

PARAMETRIC frequency conversion processes in semiconductor waveguides hold considerable promise for the formation of compact all-optical devices suitable for photonic integrated circuits. This is made possible by the large nonlinear coefficients of semiconductors in comparison with other crystals such as periodically poled lithium niobate (PPLN) [1]. Furthermore, the mature fabrication technology for AlGaAs enables low loss, highly confining waveguides leading to higher optical intensities and enhanced nonlinear effects. When ultra-short optical pulses are used in these highly dispersive semiconductors, the design of devices which utilize parametric processes such as second-harmonic generation (SHG) are complicated by group velocity mismatch (GVM). This is especially true when the second-harmonic wavelength lies close to a resonance peak of the nonlinear medium where the dispersion of the refractive index is large relative to the dispersion at the fundamental wavelength. The resulting temporal walk off between the input and the generated pulses can lead to lower conversion efficiency. Studies of PPLN for quasi-phase matching (QPM) when using femtosecond pulses demonstrated severe limitations posed by GVM such as pulse distortion and saturation effects [2]. Recently, GVM correction schemes such as quasi-group-velocity-matching (QGVM) [3] and noncollinear SHG [4] have been demonstrated in PPLN. In both cases, the effective interaction lengths were increased and conversion efficiencies were improved.

GaAs–AlAs superlattices and quantum-well intermixing (QWI) have been used to make domain-disordered QPM waveguides [5]–[7]. In this scheme, the second-order nonlinear coefficient $\chi^{(2)}$ is periodically modulated between a high value in the as-grown domains and a low value (ideally zero) in the disordered domains. The amount of back-conversion is limited when the fundamental and second-harmonic are out of phase which in turn leads to net increase of the second-harmonic. For this technique to be effective, the photon energy of the fundamental is set just below the half-bandgap resonance where the nonlinear coefficients are large while limiting two-photon absorption (TPA). Domain-disordered structures have steadily improved in performance by improving fabrication processes. Further design optimization could be realized with comprehensive modeling that includes effects such as linear loss, third-order nonlinearities, and GVM. The inherent birefringence in superlattice waveguides has highlighted the necessity of taking GVM into account when analyzing cross-phase modulation between two differently polarized modes [8]. By analyzing the impact of GVM in QPM structures fabricated in semiconductor superlattices, schemes such as QGVM could be used to improve efficiency. Optimization of the conversion efficiency is required to enable devices such as integrated self-pumped optical parametric oscillators and monolithic low-power frequency conversion devices.

Domain disordering a superlattice introduces several other unique challenges when designing QPM structures using this technique. While the purpose of QWI is to introduce a periodic modulation in the magnitude of $\chi^{(2)}$, the linear refractive index is also modified. This requires the duty cycle between the as-grown and disordered regions to be asymmetric. Deviation from the ideal duty cycle results in an accumulated phase mismatch as the fundamental and second-harmonic propagate through the structure. In practice, achieving the ideal duty cycle is complicated by the resolution of the QWI process [9]. Modulation of the linear index also leads to a process known as

Manuscript received September 21, 2007; revised October 29, 2007. This work was supported in part by the National Science and Engineering Research Council of Canada Special Research Opportunities Grant SROPJ 342462-07 and Discovery Grant 293258/5.

The authors are with the Edward S. Rogers Sr. Department of Electrical and Computer Engineering, University of Toronto, Toronto, ON M5S 3G4, Canada (e-mail: sean.wagner@utoronto.ca).

Digital Object Identifier 10.1109/JQE.2007.914884

grating assisted phase matching (GAPM) [10] which can interfere with the QPM process. Furthermore, the second-order nonlinearity cannot be completely suppressed by intermixing the superlattice. Back conversion of the second-harmonic occurs in the disordered domains of the QPM grating and reduces the overall conversion efficiency. Additionally, third-order nonlinear effects such as self-phase modulation (SPM) and TPA may disrupt the conversion process. Both effects have been experimentally measured for a GaAs–AlAs superlattice and SPM was found to be about three orders of magnitude larger than in PPLN [8]. In order to analyze the behavior of QPM with all of these effects acting simultaneously, numerical methods must be employed.

In this paper, we model the effects of third-order nonlinearities, GVM, variations in grating duty cycle, $\chi^{(2)}$ modulation depth, and GAPM on the SHG efficiency in domain-disordered QPM superlattice waveguides by computer simulations. We show good agreement with experimental results and analyze the impact of each effect on the amount of second-harmonic generated. By having a more complete model, we identify routes to optimize the QPM structure for improved conversion efficiency.

II. Theory and Modeling

In straight waveguides, it is not necessary to simulate all three dimensions under the assumption that linear and nonlinear effects are weak and do not to disrupt the transverse mode profile. In addition, the refractive index modulation in the waveguides studied due to periodic disordering are on the order of 0.05 for second-harmonic wavelengths around 775 nm which is a sufficiently small percentage of the refractive index such that the mode profiles are not disrupted. This yields several simplifications that reduce computation time. Solving Maxwell's equations under the slowly varying envelope approximation gives rise to the following coupled equations for SHG [2]:

$$\frac{\partial A_{2\omega}}{\partial z} = -j\kappa |A_\omega|^2 \exp[j\Delta k z] - \frac{1}{v_{g,2\omega}}\frac{\partial A_{2\omega}}{\partial t} - \frac{\alpha_{0,2\omega}}{2}A_{2\omega} - \left[\frac{\alpha_{2,2\omega}}{2} - j\frac{2\pi n_{2,2\omega}}{\lambda_{2\omega}}\right]\frac{|A_{2\omega}|^2}{A^{(3)}_{\text{eff},2\omega}}A_{2\omega} \tag{1}$$

$$\frac{dA_\omega}{dz} = -j\kappa A^*_\omega A_{2\omega}\exp[-j\Delta k z] - \frac{1}{v_{g,\omega}}\frac{dA_\omega}{dt} - \frac{\alpha_{0,\omega}}{2}A_\omega - \left[\frac{\alpha_{2,\omega}}{2} - j\frac{2\pi n_{2,\omega}}{\lambda_\omega}\right]\frac{|A_\omega|^2}{A^{(3)}_{\text{eff},\omega}}A_\omega \tag{2}$$

where $A_{2\omega}$ is the pulse envelope of the second-harmonic, A_ω is the pulse envelope of the fundamental, $v_{g,i}$ are the group velocities, $\alpha_{0,i}$ are the linear loss coefficients, Δk is the wavenumber mismatch, and z is the propagation distance. The pulse envelopes are normalized such that the fundamental and second-harmonic powers are $P = |A|^2$. The coupling coefficient, κ, is defined as

$$\kappa = \frac{\pi\chi^{(2)}_{\text{eff}}}{\lambda_\omega}\sqrt{\frac{2}{n^2_\omega n_{2\omega} c\varepsilon_0 A^{(2)}_{\text{eff}}}} \tag{3}$$

where $\chi^{(2)}_{\text{eff}}$ is the effective second-order nonlinear coefficient. Spatial distributions of the waveguide modes are accounted for in the effective second-order overlap area defined by

$$A^{(2)}_{\text{eff}} = \frac{\left[\int_{-\infty}^{\infty}\int_{-\infty}^{\infty}|F_{2\omega}|^2 dxdy\right]\left[\int_{-\infty}^{\infty}\int_{-\infty}^{\infty}|F_\omega|^2 dxdy\right]^2}{\left[\int_{-\infty}^{\infty}\int_{-\infty}^{\infty}F_{2\omega}|F_\omega|^2 dxdy\right]^2} \tag{4}$$

where $F_{2\omega}$ and F_ω are the transverse mode profiles for the second-harmonic and fundamental respectively. SPM and TPA are modeled in (1) and (2) by coefficients n_2 and α_2 respectively, and the third-order effective areas $A^{(3)}_{\text{eff}}$, which is defined in [8]. Values for these coefficients were obtained previously for 14:14 monolayer GaAs–AlAs superlattice-core waveguides at wavelengths around 1550 nm [8]. All of the above parameters are different for the as-grown and disordered superlattice. Most notably, Δk varies along z due to modulation of the linear index, and $\chi^{(2)}_{\text{eff}}$ varies along z as intended for the QPM process. However, these changes are small enough that the slowly varying amplitude approximation still applies, thus (1) and (2) remain valid.

The QPM waveguide was discretized into segments of either as-grown or disordered material. Equations (1) and (2) were then solved numerically using the split-step Fourier method [11]. Simulations were run such that the fundamental pulse peak remained at $t = 0$ and the generated second-harmonic pulse was allowed to drift in relative to the fundamental according to the difference in the group velocities.

The waveguide structure modeled is based on a 14:14 monolayer GaAs–AlAs superlattice core layer which was optimized to give a maximal modulation and end-fire coupling efficiency [12]. Effective refractive index measurements were previously reported for this structure [13] and were used to calculate the waveguide mode profiles and QPM period lengths. For 3.0 μm-wide and 0.8 μm-deep rib waveguides, the effective overlap area between a 1550 nm fundamental and 775 nm second-harmonic was calculated by (4) as 12 μm^2 using mode profiles generated by Lumerical MODE Solutions software. For the Type-I SHG interaction (TE fundamental, TM second-harmonic), $\chi^{(2)}_{\text{eff}} = \chi^{(2)}_{zxy}$ and was set to the theoretical value of 125 pm/V for the as-grown superlattice and 80 pm/V in disordered superlattice [14]. Group velocity values were calculated from the effective index dispersion curves and the GVM parameters are defined as

$$\delta u = \frac{1}{v_{g,\omega}} - \frac{1}{v_{g,2\omega}}. \tag{5}$$

This gives estimated GVM parameter values of $\delta u_0 = 2.44 \times 10^{-9}$ s/m for as-grown domains and $\delta u_0 = 2.06 \times 10^{-9}$ s/m disordered domains. Linear loss coefficients for the fundamental were set to 3.5 cm^{-1} for as-grown segments and 7.5 cm^{-1} for disordered segments. For the second-harmonic, loss coefficients were estimated for as-grown and disordered segments as 35 and 75 cm^{-1}, respectively. A QPM period of 3.7 μm was calculated from the coherence lengths

$$L_c = \frac{\lambda_\omega}{4\Delta n} \tag{6}$$

where $\Delta n = n_{2\omega} - n_{\omega}$ is the difference in the effective indexes for the second-harmonic and fundamental waves. The coherence lengths for as-grown and disordered segments were 1.7 and 2.0 μm, respectively, which yields an ideal duty cycle of 45:55 in the QPM period. Grating lengths of 200 QPM periods were used, giving a propagation length of 740 μm.

For all simulations, the fundamental wavelength was set to 1550 nm, which falls below the half-bandgap resonance of the superlattice. The input fundamental peak power was set to 25 W such that the output fundamental average power was on the order of milliwatts, similar to experiments with actual QPM waveguides. Gaussian pulses were used and set to a full-width at half-maximum (FWHM) duration of 1.3 ps. These values mimic our experimental setup and samples [7].

III. Results

A. Third-Order Nonlinear Effects

Third-order nonlinear effects, such as SPM and TPA, were examined for their impact on the conversion efficiency. The effective nonlinear coefficients for the fundamental in the as-grown regions were set to $n_2 = 2.5 \times 10^{-13}$ cm^2/W and $\alpha_2 = 1.4$ cm/GW. In the disordered domains, n_2 was set to be an order of magnitude smaller than in as-grown regions as is expected from theoretical calculations [14]. Disordering the superlattice should also shift the TPA peak at least 100 nm below the fundamental wavelength and thus α_2 was set to zero in disordered domains. Other parameters were set to their nominal values.

Fig. 1 shows the normalized SHG conversion efficiency as the input fundamental peak power is increased. In the case where both SPM and TPA were set to zero, the efficiency reduced solely due to depletion of the fundamental by the conversion process. Adding either TPA or SPM had a similar impact on the conversion efficiency, reducing it by as much as 24% at 250 W of input power. At lower powers, TPA attenuates the fundamental and has a larger effect on the efficiency than SPM does. Above 150 W, nonlinear phase shifts and spectral broadening disturb the phase matching process and SPM dominates in dropping the conversion efficiency. With both effects included simultaneously, the conversion efficiency drops by $\sim 33\%$ for an input peak power of 250 W. The TPA portion of the efficiency drop could potentially be eliminated by operating the fundamental further below the half-bandgap to avoid the tail of the TPA peak or by redesigning the superlattice structure to adjust the location of the half-bandgap. However, n_2 will remain and limits the maximum amount of fundamental power that can be used. At peak powers below 50 W, the impact of SPM and TPA is less than 1%. In subsequent simulations where other phenomena were examined, the input peak power was kept at 25 W to limit third-order effects. It is worth noting the limitation on the QPM efficiency due to third-order effects, which this section highlights. Because the bandgap modulation is central to the modulation of the second-order nonlinearity, there exists a requirement to work as close as possible to a resonance. However as can be seen in this section, this is accompanied by another limitation caused by third-order effects which sets in near the optimum operating regime favorable for maximum modulation in the second-order nonlinearity.

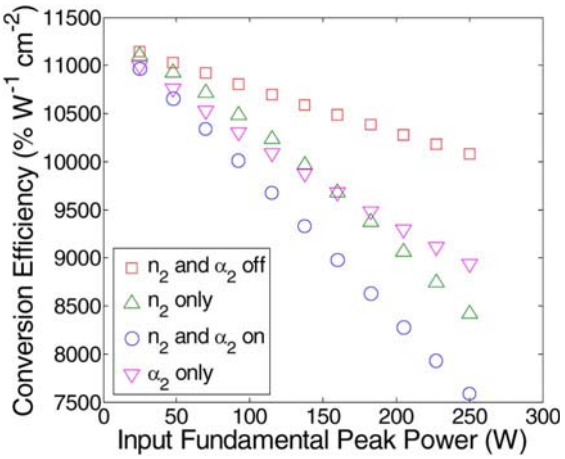

Fig. 1. Effect of SPM (n2) and TPA (a2) on the normalized conversion efficiency as the input fundamental peak power is increased.

B. Group-Velocity Mismatch

GVM will limit the amount of conversion to the second-harmonic by causing the generated pulse to walkoff from the input fundamental. To study this effect, the ideal QPM duty cycle was simulated with varying levels of GVM. An accurate account of the GVM in dispersive media such as GaAs–AlGaAs semiconductors is difficult to obtain. Therefore, the GVM is varied here in both directions around the best estimate. Fig. 2 shows the generated second-harmonic pulse energy over propagation through 200 QPM periods. Output average powers are on the order of microwatts for a 80-MHz pulse repetition rate, which agrees with actual experimental results to within an order of magnitude [7]. At the estimated GVM values for the actual structure modeled, the second-harmonic pulse energy is reduced by $\sim 23\%$ over the case where GVM is zero. If the GVM is twice as large as was calculated, the second-harmonic generated drops further to nearly 50% of the ideal.

Peak second-harmonic powers were generated at a propagation length shorter than the total length of the simulated structure. In the case where $\delta u = \delta u_0$, this peak occurs after a length of 585 μm. This is longer than the walkoff length of 350 μm calculated using $L_w = \tau/\delta u$ where τ is the $1/e$ pulse length of the fundamental [15]. This shows that the walkoff length is not necessarily the optimal QPM device length. Output second-harmonic pulse shapes are shown in Fig. 3. The half-maximum point on the leading edge of the pulse for the $\delta u = \delta u_0$ case is $\sim 47\%$ of the FWHM. This distortion is minimal when compared with the $2\delta u_0$ case and shows that allowing the interaction to proceed past the walkoff length is not detrimental. After the peak shown in Fig. 2, further walkoff reduces the interaction and second-harmonic power is decreased through linear loss. Furthermore, linear losses in the fundamental stalls the interaction and hence the appearance of a peak even in the case where GVM is zero.

A graph such as Fig. 2 is pivotal when choosing the optimal QPM grating length. At the peak point identified, the second-harmonic and fundamental pulses should be selectively delayed

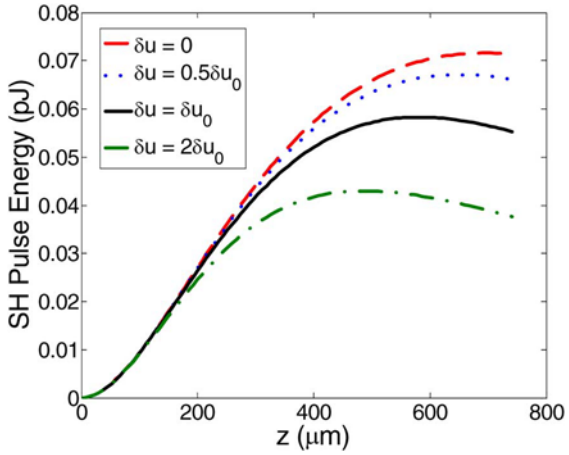

Fig. 2. Second-harmonic pulse energy generated over propagation distance for the 45:55 duty cycle at different values for the GVM parameter with 25-W peak fundamental power.

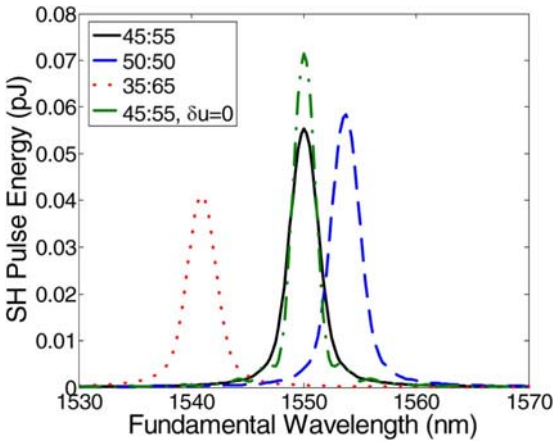

Fig. 4. SHG tuning curves for a QPM period of 3.7 μm with duty cycles of 45:55, 50:50, and 35:65. The tuning curve for the 45:55 duty cycle without GVM effects is also included. Peak input power was 25 W.

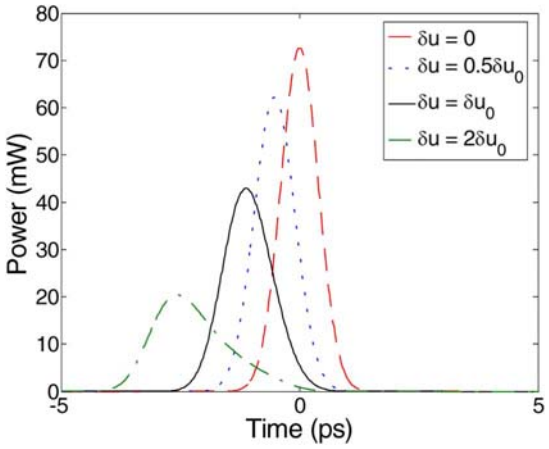

Fig. 3. Generated second-harmonic pulses for different values of the GVM parameter with 25-W peak fundamental power.

to realign their peaks as is done in the QGVM scheme. Another possible method for improving the efficiency would be to tailor the group index by using highly confining waveguide structures such as photonic nanowires [16]. However, this solution requires delicate balancing between the GVM parameter and the increased scattering losses of deeply etched waveguides.

C. Duty Cycle Variations

Fabrication tolerances of QWI technology provide imperfect control over the duty cycle of the domains. This is governed by the type of QWI technology. For example, lateral diffusion of lattice constituents is more dominant in impurity free vacancy disordering (IFVD) [17] techniques than in ion implantation. While studies conducted previously suggest that ion implantation has better resolution [18], deviations greater than 10% in the designed duty cycle are likely. As such, variation in the QPM duty cycle was explored in our simulations.

In general, the QPM period can be calculated as

$$\Lambda = \frac{\lambda_\omega}{2\left[a\Delta n_1 + (1-a)\,\Delta n_2\right]} \tag{7}$$

where the duty cycle between the domains is $a : (1 - a)$. In the case where $\Delta n_1 = \Delta n_2$, (7) becomes $\Lambda = \lambda_\omega / 2\Delta n$ and the period does not depend on the duty cycle. As this is not the case for the superlattice studied, the peak conversion wavelength for a given QPM period length will be different for different duty cycles.

Tuning curves from simulations for duty cycles of 45:55, 50:50, and 35:65 are shown in Fig. 4 with GVM and linear loss included. A red-shift in the peak wavelength of about 4 nm results for the 50:50 case and a blue-shift of 9 nm happens for the 35:65 case. The 50:50 duty cycle outperformed the ideal duty cycle at its respective peak wavelength. This was due to reduced losses in the shorter disordered domains of the 50:50 structure. Without linear losses included in the simulations, the 45:55 duty cycle outperformed the 50:50 duty cycle which has a reduced gain due to shorter as-grown domains where $\chi^{(2)}$ is larger. The 35:65 duty cycle remained as the lowest performing structure with or without linear loss since the more strongly nonlinear as-grown domains are shorter and the lossy disordered domains are longer than in the other two structures. The spectral bandwidth was ~ 3 nm for all of the curves. When the GVM was set to zero the bandwidth was reduced to about 2.3 nm for the 45:55 case. This was explained by the temporal walkoff which limits the amount of back-conversion at nearly phase matched wavelengths on either side of the peak.

D. Modulation Depth of Nonlinear and Linear Properties

The size of the differential shift in $\chi^{(2)}$ between as-grown and disordered domains depends greatly on the QWI process. Photoluminescence measurements of QPM samples made using ion-implantation indicated that the bandgap shift in the disordered regions was only half of what is theoretically possible for a 14:14 GaAs–AlAs superlattice [18]. With less bandgap shift, the change in $\chi^{(2)}$ will also be less. Thus, different levels of modulation in $\chi^{(2)}$ were investigated to determine the impact of incomplete disordering of the superlattice in the disordered domains.

As-grown domains were set to have the theoretical $\chi^{(2)}$ value of 125 pm/V. In disordered domains, $\chi^{(2)}$ was set to different

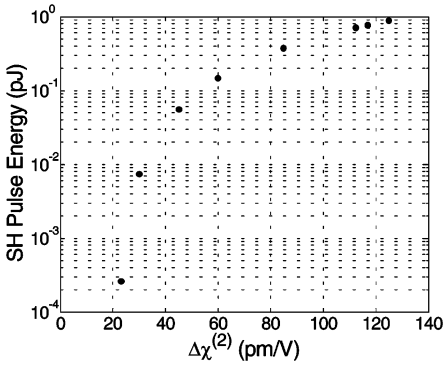

Fig. 5. Output second-harmonic pulse energy for different values of in the disordered domains of the QPM grating. The expected is 45 pm/V. Peak input power was 25 W.

levels to simulate various degrees of modulation. GVM values were set to δu_0 and linear losses were included in all simulations. As shown in Fig. 5, the expected change in $\chi^{(2)}$ of 45 pm/V reduces the amount of second-harmonic energy to about 6% of what would be generated in the ideal case where $\chi^{(2)} = 0$ in disordered regions. In the cases where the $\chi^{(2)}$ is reduced to an order of magnitude below the theoretical values for as-grown and disordered superlattice, the reduction in efficiency is less than 20%. If the superlattice is not completely disordered such that $\Delta\chi^{(2)}$ is half of what is expected, the second-harmonic energy generated is reduced by over two orders of magnitude compared to the case where complete disordering is achieved. This emphasizes the need to optimize the QWI process to yield complete intermixing in disordered regions.

Periodic modulation of the linear index has a similar effect on the coupling coefficient of (3) as modulation of $\chi^{(2)}$. Thus, linear index changes influence the power flow between the fundamental and second-harmonic by the GAPM process. For the superlattice waveguides, index changes of 0.045 at the second-harmonic and 0.01 at the fundamental raised κ by $\sim 1\%$ in the disordered regions, leading to more backconversion to the fundamental. In all previous results, the modulation was included and GAPM was affecting the SHG process. To isolate the impact of GAPM, the refractive indexes in (3) were held constant throughout the QPM structure and only $\chi^{(2)}$ was allowed to modulate κ. The resulting output second-harmonic pulse energies were found to be $\sim 7\%$ larger in this non-GAPM case over the GAPM case. Compared with incomplete modulation of $\chi^{(2)}$, GAPM introduces only a small efficiency drop. However, this efficiency loss may be regained with optimization of the waveguide design to lessen the change in the effective index between as-grown and disordered segments.

IV. Conclusions

In conclusion, the effects of GVM, duty cycle, and $\chi^{(2)}$ modulation on SHG in superlattice QPM waveguides have been analyzed by computer simulations. Output second-harmonic powers from the simulations agree within an order of magnitude with actual experimental results. SPM and TPA both led to drops in conversion efficiency of up to 33% as the input fundamental peak power was increased. Large reductions in conversion efficiency result from temporal walkoff and incomplete disordering. Optimal QPM grating lengths for maximum conversion were identified which did not correspond to the walkoff length. Variations in the duty cycle shift the tuning curve and GVM broadens the spectral bandwidth by reducing back conversion at nearly phase-matched wavelengths. Maximal modulation of $\chi^{(2)}$ by complete intermixing was found to be necessary for optimal conversion. Modulation in the linear index led to GAPM and an efficiency reduction of $\sim 7\%$. Similar consequences are expected for other three-wave mixing processes such as sum- and difference-frequency mixing. With more data on the waveguide characteristics and on fabrication tolerances, optimal domain-disordered QPM waveguides can be designed and modeled to give more efficient frequency conversion devices.

Acknowledgment

The authors thank Prof. D. C. Hutchings of the University of Glasgow, Glasgow, U.K., for useful discussions.

References

[1] T. Skauli, K. L. Vodopyanov, T. J. Pinguet, A. Schober, O. Levi, L. A. Eyres, M. M. Fejer, J. S. Harris, B. Gerard, L. Becouarn, E. Lallier, and G. Arisholm, "Measurement of the nonlinear coefficient of orientation-patterned GaAs and demonstration of highly efficient second-harmonic generation," *Opt. Lett.*, vol. 27, pp. 628–630, 2002.

[2] Z. Zheng, A. M. Weiner, K. R. Parameswaran, M.-H. Chou, and M. M. Fejer, "Femtosecond second-harmonic generation in periodically poled lithium niobate waveguides with simultaneous strong pump depletion and group-velocity walk-off," *J. Opt. Soc. Amer. B*, vol. 19, pp. 839–848, 2002.

[3] X. Xie, J. Huang, and M. M. Fejer, "Narrow-linwidth near-degenerate optical parametric generation achieved with quasi-group-velocity-matching in lithium niobate waveguides," *Opt. Lett.*, vol. 31, pp. 2190–2192, 2006.

[4] N. Fujioka, S. Ashihara, H. Ono, T. Shimura, and K. Kuroda, "Group-velocity-matched noncollinear second-harmonic generation in quasi-phase matching," *J. Opt. Soc. Amer. B*, vol. 22, pp. 1283–1289, 2005.

[5] A. S. Helmy, D. C. Hutchings, T. C. Kleckner, J. H. Marsh, A. C. Bryce, J. M. Arnold, C. R. Stanley, J. S. Aitchison, C. T. A. Brown, K. Moutzouris, and M. Ebrahimzadeh, "Quasi phase matching in GaAs-AlAs superlattice waveguides through bandgap tuning by use of quantum-well intermixing," *Opt. Lett.*, vol. 25, pp. 1370–1372, 2000.

[6] K. Zeaiter, D. C. Hutchings, R. M. Gwilliam, K. Moutzouris, S. V. Rao, and M. Ebrahimzadeh, "Quasi-phase-matched second-harmonic generation in a GaAs–AlAs superlattice waveguide by IoN-implantation-induced intermixing," *Opt. Lett.*, vol. 28, pp. 911–913, 2003.

[7] D. C. Hutchings, M. Sorel, K. Zeaiter, A. J. Zilkie, B. Leesti, A. Saher-Helmy, P. W. E. Smith, and J. S. Aitchison, "Quasi-phase-matched second harmonic generation with picosecond pulses in GaAs–AlAs superlattice waveguides," presented at the Nonlinear Guided Waves (NLGW), Toronto, ON, Canada, 2004.

[8] S. J. Wagner, J. Meier, A. S. Helmy, J. S. Aitchison, M. Sorel, and D. C. Hutchings, "Polarization-dependent nonlinear refraction and two-photon absorption in GaAs–AlAs superlattice waveguides below the half-bandgap," *J. Opt. Soc. Amer. B*, vol. 24, pp. 1557–1563, 2007.

[9] A. S. Helmy, A. C. Bryce, D. C. Hutchings, J. S. Aitchison, and J. H. Marsh, "Band gap gratings using quantum well intermixing for quasi-phase-matching," *J. Appl. Phys.*, vol. 100, pp. 123107–8, 2006.

[10] M. M. Fejer, G. A. Magel, D. H. Jundt, and R. L. Byer, "Quasi-phase-matched second harmonic generation: Tuning and tolerances," *IEEE J. Quantum Electron.*, vol. 28, pp. 2631–2654, 1992.

[11] G. P. Agrawal, *Nonlinear Fiber Optics*, 2nd ed. San Diego, CA: Academic, 1995.

[12] D. C. Hutchings and T. C. Kleckner, "Quasi phase matching in semiconductor waveguides by intermixing: Optimization considerations," *J. Opt. Soc. Amer. B*, vol. 19, pp. 890–894, 2002.

[13] T. C. Kleckner, A. S. Helmy, K. Zeaiter, D. C. Hutchings, and J. S. Aitchison, "Dispersion and modulation of the linear optical properties of GaAs-AlAs superlattice waveguides using quantum-well intermixing," *IEEE J. Quantum Electron.*, vol. 42, no. 3, pp. 280–286, Mar. 2006.

[14] D. C. Hutchings, "Theory of ultrafast nonlinear refraction in semiconductor superlattices," *IEEE J. Sel. Top. Quantum Electron.*, vol. 10, no. 5, pp. 1124–1132, Sep./Oct. 2004.
[15] G. Imeshev, M. A. Arbore, M. M. Fejer, A. Galvanauskas, M. Fermann, and D. Harter, "Ultrashort-pulse second-harmonic generation with longitudinally nonuniform quasi-phase-matching gratings: Pulse compression and shaping," *J. Opt. Soc. Amer. B*, vol. 17, pp. 304–318, 2000.
[16] A. C. Turner, C. Manolatou, B. S. Schmidt, M. Lipson, M. A. Foster, J. E. Sharping, and A. L. Gaeta, "Tailored anomalous group-velocity dispersion in silicon channel waveguides," *Opt. Exp.*, vol. 14, pp. 4357–4362, 2006.
[17] J. H. Marsh, "Quantum well intermixing," *Semicond. Sci. Technol.*, vol. 6, pp. 1136–1155, 1993.
[18] P. Scrutton, M. Sorel, D. C. Hutchings, J. S. Aitchison, and A. S. Helmy, "Characterizing bandgap gratings in GaAs:AlAs superlattice structures using interface phonons," *IEEE Photon. Technol. Lett.*, vol. 19, no. 9, pp. 677–679, May 2007.

Sean J. Wagner (S'98–M'08) received the B.A.Sc. degree in computer engineering from University of Waterloo, Waterloo, ON, Canada, in 2003, and the M.A.Sc. degree from the University of Toronto, Toronto, ON, Canada, in 2006 where his research included characterizing the nonlinear properties of semiconductor superlattice waveguides and devices, where he is currently working toward the Ph.D. degree in the Edward S. Rogers Sr. Department of Electrical and Computer Engineering.

He has held positions at IBM Canada and Philips Analytical (a former division of Royal Philips Electronics). His most recent position was with Evertz Microsystems Inc., Burlington, ON, Canada where he developed fiber optic equipment. His research interests include nonlinear optics, all-optical switching and signal processing, and monolithic integration techniques for optical and optoelectronic components in semiconductors.

Mr. Wagner is a student member of Optical Society of America and SPIE.

Ahmed Al Muhairi (S'07) is currently an undergraduate student in the Engineering Science (Physics Option) program at the University of Toronto, Toronto, ON, Canada.

His current research topics of interest are nonlinear optics and quantum optics.

J. Stewart Aitchison (M'96–SM'00) received the B.S. and Ph.D. degrees in physics from Heriott-Watt University, Edinburgh, U.K., in 1984 and 1987, respectively.

He is currently the Vice Dean of Research of the Faculty of Applied Science and Engineering, University of Toronto, Toronto, ON, Canada. He also holds the Nortel Institute Chair in Emerging Technology at the University of Toronto. He has seven patents, more than 100 journal publications, and 200 conference presentations to his credit. His research interests include all-optical switching and signal processing, optoelectronic integration, and optical biosensors.

Dr. Aitchison is a member of the Optical Society of America and a Fellowof the Institute of Physics, London, U.K.

Amr S. Helmy (M'99–SM'06) received the B.Sc. degree in electronics and telecommunications engineering from Cairo University, Cairo, Egypt, in 1993, and the M.Sc. and Ph.D. degrees with a focus on photonic fabrication technologies from the University of Glasgow, Glasgow, U.K., in 1994 and 1999, respectively.

Prior to his academic career, he held a position at Agilent Technologies Photonic Devices, R&D Division, U.K., where his responsibilities included developing distributed feedback lasers, monolithically integrated lasers, modulators, and amplifiers in InP-based semiconductors. He also developed high-powered submarine-class 980-nm InGaAs pump lasers. He is currently an Assistant Professor in the Department of Electrical and Computer Engineering, University of Toronto, Toronto, ON, Canada. His research interests include photonic device physics and characterization techniques, with emphasis on nonlinear optics in III–V semiconductors; applied optical spectroscopy in III-V optoelectronic devices andmaterials; and III–V fabrication and monolithic integration techniques.

Dr. Helmy is a member of the Optical Society of America.